Influence of miscible viscous fingering of finite slices on an adsorbed solute dynamics

M. Mishra,[1] M. Martin,[2] and A. De Wit[1]
[1]*Nonlinear Physical Chemistry Unit and Center for Nonlinear Phenomena and Complex Systems, Service de Chimie Physique et Biologie Théorique, Université Libre de Bruxelles (ULB), CP 231, 1050 Brussels, Belgium*
[2]*Ecole Supérieure de Physique et de Chimie Industrielles, Laboratoire de Physique et Mécanique des Milieux Hétérogènes (PMMH), UMR 7636 CNRS, Université Paris 6, Université Paris 7, 10 Rue Vauquelin, 75231 Paris Cedex 05, France*

(Received 7 April 2009; accepted 25 June 2009; published online 5 August 2009)

Viscous fingering (VF) between miscible fluids of different viscosities can affect the dispersion of finite width samples in porous media. We investigate here the influence of such VF due to a difference between the viscosity of the displacing fluid and that of the sample solvent on the spatiotemporal dynamics of the concentration of a passive solute initially dissolved in the injected sample and undergoing adsorption on the porous matrix. Such a three component system is modeled using Darcy's law for the fluid velocity coupled to mass-balance equations for the sample solvent and solute concentrations. Depending on the conditions of adsorption, the spatial distribution of the solute concentration can either be deformed by VF of the sample solvent concentration profiles or disentangle from the fingering zone. In the case of deformation by fingering, a parametric study is performed to analyze the influence of parameters such as the log-mobility ratio, the ratio of dispersion coefficients, the sample length, and the adsorption retention parameter k' on the widening of the solute concentration peak. The results highlight experimental evidences obtained recently in reversed-phase liquid chromatography. © *2009 American Institute of Physics*.
[DOI: 10.1063/1.3200870]

I. INTRODUCTION

Miscible viscous fingering (VF) is an interfacial fluid flow instability that occurs when a less viscous fluid displaces another more viscous miscible one in a porous medium, leading to the formation of fingerlike patterns at the interface of both fluids.[1] VF of one single interface impacts a variety of practical applications such as oil recovery, filtration, or hydrology for instance and has been the subject of numerous investigations over the years since the pioneering work of Hill[2] and Saffman and Taylor.[3]

VF has also been observed in liquid chromatography, which is used to separate the chemical components of a given sample by passing it through a column of porous medium.[4–12] VF also influences the spreading of finite width samples in localized pollution zones in aquifers.[12,13] In the case of such viscous slices of finite extent, fingering is a transient phenomenon as the mixing of both sample and carrier fluids leads to an effective decrease in time of the log-mobility ratio. Even though the spreading of the sample may look like Gaussian at long times when dispersion becomes again dominant in the transport phenomena, the variance of the peak is larger than expected because of fingering at earlier time. A quantitative characterization of the contribution of such VF in the variance of the peaks has been conducted in the frame work of chromatographic[11,12] or pollution applications.[12] This widening has been shown to be of larger extent when the sample is less viscous than the carrier fluid than when it is more viscous.[14]

In chromatography and for problems of transport in aquifers, the finite size of the viscous sample and the solute adsorption on the porous matrix can be of importance.[10,15,16] Recently, a theoretical model taking into account such adsorption of the species ruling the viscosity of the solution during miscible VF of finite width samples was developed by Mishra *et al.*[17] The growth rates of the unstable wave numbers of the VF instability have been discussed by means of a linear stability analysis limited to the initial stage of development of the instability. On later stages, nonlinear dynamics have been analyzed by means of numerical simulations when the viscosity-modifying component in the sample is retained or not. When this component is retained, its effect is similar to that of an unretained solute with a $(1+k')$ smaller viscosity, where k' is the retention factor. The typical width of the fingers is also decreased by a factor $(1+k')$.

In chromatography, this situation can occur for polymeric solutes of relatively large molar mass as the intrinsic viscosity of polymers increases with their molar mass. In most liquid chromatographic analyses, the sample solutes have however a relatively low molar mass, hence a too low intrinsic viscosity to induce a VF phenomenon affecting dispersion characteristics. However, in order to increase the solubility of the components to be analyzed, the solutes are often diluted in a solvent whose chemical nature and hence viscosity differ from those of the displacing fluid. Then, VF may develop at the unstable sample solvent/eluent interface and affect the retained solute zones. Experimental evidences that the chromatographic peak shapes of solutes eluted under reversed-phase liquid chromatographic conditions are sig-

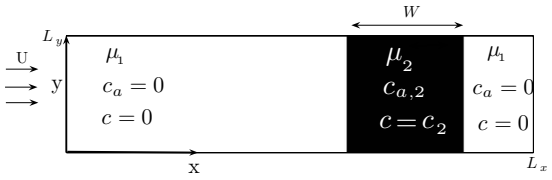

FIG. 1. Sketch of the system at initial time.

nificantly dependent on the nature and/or composition of the sample solvent have been given recently.[10] This phenomenon has been clearly associated with the difference between the eluent and sample solvent viscosities. To our knowledge, there is no quantitative study or any modeling of the influence of VF on the shape of the chromatographic peaks of solutes in this situation which typically involves three components: the eluent (or displacing fluid), the sample solvent, and the retained solute.

In this context, the purpose of the present study is to understand how a VF instability occurring between the displacing fluid and the (unretained) sample solvent affects the spatiotemporal distribution of a retained solute initially dissolved in the solvent and to study the influence of the extent of retention on the solute concentration dynamics.

We construct a model for miscible VF of a three component system, considering the dynamics of the carrier fluid and of both a solute and a solvent in the sample, incorporating a linear adsorption isotherm for the solute. This model couples Darcy's law for the evolution of the flow velocity with an equation describing the evolution of the concentration of the sample solvent and with a mass-balance equation for the solute concentration. This solute undergoes adsorption-desorption processes on the porous matrix. Numerical simulations are performed with a viscosity-modifying sample solvent and retained solutes. The results are discussed in terms of a retention parameter k' quantifying the adsorption phenomena. Theoretical explanations of the disengagement of solute and sample solvent peak shapes are also presented for a pure dispersive case.

The article is organized as follows: in Sec. II, we introduce our three component model while in Sec. III, we describe our numerical integration method. Results are described in Sec. IV before conclusions are drawn in Sec. V.

II. THREE COMPONENT MODEL

The system considered (see Fig. 1) is a two dimensional (2D) porous medium of length L_x and width L_y in which a sample consisting of a solute or analyte in concentration $c_{a,2}$ dissolved in a sample solvent of concentration c_2 and of viscosity μ_2 is injected at an initial time $t=0$. The initial length of the sample is W. This sample is displaced by another miscible fluid, the carrier fluid or eluent, different from the sample solvent which has a viscosity $\mu_1 < \mu_2$ and in which the sample solvent concentration $c=0$ and the solute concentration is $c_{a,2}=0$. The displacing fluid is injected uniformly with a mean velocity U along the x direction.

We assume that the initial solute or analyte concentration $c_{a,2}$ in the sample solvent is small and does not influence the viscosity of the fluids. This viscosity is however assumed to depend on the concentration of the sample solvent c through an exponential function,

$$\mu(c) = \mu_1 e^{R(c/c_2)}, \tag{1}$$

where the log-mobility ratio R is defined as $R=\ln(\mu_2/\mu_1)$. If $\mu_2 > \mu_1$, $R>0$, and the rear interface of the sample where the less viscous displacing fluid pushes the more viscous sample is unstable with regard to VF. The frontal interface is on the contrary stable. As the solute does not impact the viscosity of the solutions, it will behave as a passive scalar in the flow. The spatiotemporal dynamics of this solute's concentration depends however on adsorption on the porous matrix.

Once the sample is injected in the porous matrix the solute can adsorb onto the porous matrix following the reversible adsorption-desorption reaction:

$$c_{a,m} \underset{k_d}{\overset{k_a}{\rightleftharpoons}} c_{a,s}. \tag{2}$$

Here $c_{a,m}$ and $c_{a,s}$ are the concentration of the solute in the mobile and stationary phases, respectively, while k_a and k_d are the adsorption and desorption kinetic constants.

Assuming that the fluid is incompressible and the flow inside the porous medium is governed by Darcy's law (4), the governing equations for the system are as follows:

$$\underline{\nabla} \cdot \underline{u} = 0, \tag{3}$$

$$\underline{\nabla} p = -\frac{\mu(c)}{K_p}\underline{u}, \tag{4}$$

$$\frac{\partial c}{\partial t} + \underline{u} \cdot \underline{\nabla} c = D_x \frac{\partial^2 c}{\partial x^2} + D_y \frac{\partial^2 c}{\partial y^2}, \tag{5}$$

$$\frac{\partial c_{a,m}}{\partial t} + F\frac{\partial c_{a,s}}{\partial t} + \underline{u} \cdot \underline{\nabla} c_{a,m} = D_{a_x} \frac{\partial^2 c_{a,m}}{\partial x^2} + D_{a_y} \frac{\partial^2 c_{a,m}}{\partial y^2}, \tag{6}$$

where $\underline{u}=(u,v)$ is the 2D fluid velocity with u and v the velocity components in the x and y directions, respectively, K_p is the permeability of the porous medium, and p is the pressure. Equation (5) is the convection-diffusion equation for the concentration c of the sample solvent ruling the viscosity of the solution. Equation (6) is the mass-balance equation for the solute concentration c_a, where $F=V_s/V_m = (1-\epsilon_{\text{tot}})/\epsilon_{\text{tot}}$ is the phase ratio of the volume V_s and V_m of the stationary and mobile phases, where ϵ_{tot} is the total porosity or void volume fraction of the porous medium.[18] D_x and D_y are the dispersion coefficients of the sample solvent in the displacing fluid along the x and y directions, respectively, while D_{a_x} and D_{a_y} are those of the solute. Influence of Korteweg stresses[19–21] are here assumed negligible.

Assuming a linear isotherm adsorption dependence between the concentration $c_{a,s}$ and $c_{a,m}$ as

$$c_{a,s} = K c_{a,m}, \tag{7}$$

where $K=k_a/k_d$ is the equilibrium constant of the adsorption-desorption equilibrium (2), Eq. (6) becomes

$$(1+k')\frac{\partial c_{a,m}}{\partial t}+\underline{u}\cdot\underline{\nabla}c_{a,m}=D_{a_x}\frac{\partial^2 c_{a,m}}{\partial x^2}+D_{a_y}\frac{\partial^2 c_{a,m}}{\partial y^2}, \tag{8}$$

where $k'=FK$. Let us note that at the moment of injection, all solute or analyte molecules are in the mobile phase of volume V_m so the concentration of solute $c_{a,2}=n/V_m$, where n is the total number of analyte moles injected in the column. When the sample starts to move in the column at $t=0$ and after the adsorption/desorption equilibrium has been reached, the corresponding analyte concentration in the mobile ($c_{a,2m}$) and stationary ($c_{a,2s}$) phases are

$$c_{a,2m}=n_m/V_m,$$

$$c_{a,2s}=n_s/V_s,$$

where n_s and n_m are the number of analyte moles in the stationary and mobile phases, respectively. Hence, the conservation of the total number of solute moles $n=n_s+n_m$ along with $c_{a,2s}=Kc_{a,2m}$ implies that

$$c_{a,2}V_m=c_{a,2m}V_m+c_{a,2s}V_s=c_{a,2m}(1+k')V_m,$$

which leads to

$$c_{a,2m}=c_{a,2}/(1+k').$$

Therefore, the mobile phase concentration of the analyte $c_{a,m}$ varies from 0 in the pure eluent to $c_{a,2m}=c_{a,2}/(1+k')$ in the sample.

To nondimensionalize the governing equations, we choose the concentration c_2 and $c_{a,2}/(1+k')$ as the reference concentration for the solvent and solute concentrations, respectively, and U as the characteristic velocity. Defining a length scale $L_c=D_x/U$ and a time scale $t_c=D_x/U^2$, the nondimensional quantities are then obtained as

$$\hat{x}=\frac{x}{L_c},\quad \hat{y}=\frac{y}{L_c},\quad \hat{t}=\frac{t}{t_c},\quad \hat{u}=\frac{u}{U},$$

$$\hat{v}=\frac{v}{U},\quad p^*=\frac{p}{\mu_1 D_x/K_p},$$

$$\mu^*=\frac{\mu}{\mu_1},\quad c^*=\frac{c}{c_2},\quad c^*_{a,m}=(1+k')\frac{c_{a,m}}{c_{a,2}},$$

$$\epsilon=\frac{D_y}{D_x},\quad \epsilon_a=\frac{D_{a_y}}{D_{a_x}},\quad \delta=\frac{D_{a_x}}{D_x}.$$

Introducing a reference frame moving with the injection speed

$$x^*=\hat{x}-\hat{t},\quad y^*=\hat{y},\quad u^*=\hat{u}-1,\quad v^*=\hat{v},\quad t^*=\hat{t},$$

the governing Eqs. (3)–(5) and (8) with the concentration-dependent viscosity Eq. (1) become, after dropping the superscripts (*),

$$\underline{\nabla}\cdot\underline{u}=0, \tag{9}$$

$$\underline{\nabla}p=-\mu(c)(\underline{u}+\underline{e}_x), \tag{10}$$

$$\frac{\partial c}{\partial t}+\underline{u}\cdot\underline{\nabla}c=\frac{\partial^2 c}{\partial x^2}+\epsilon\frac{\partial^2 c}{\partial y^2}, \tag{11}$$

$$(1+k')\frac{\partial c_{a,m}}{\partial t}+(u-k')\frac{\partial c_{a,m}}{\partial x}+v\frac{\partial c_{a,m}}{\partial y}=\delta\left[\frac{\partial^2 c_{a,m}}{\partial x^2}+\epsilon_a\frac{\partial^2 c_{a,m}}{\partial y^2}\right], \tag{12}$$

$$\mu(c)=e^{Rc}. \tag{13}$$

From the above equations it is clear that Eq. (12) is decoupled from Eqs. (9)–(11). Hence, once the velocity field is determined from Eqs. (9)–(11) and (13) for given R and ϵ, the transport of the solute concentration $c_{a,m}$ can be analyzed easily for different values of the analyte parameters (k',δ,ϵ_a). Using this model, our goal is now to analyze the influence of the viscosity dependence on the sample solvent concentration c on the spatiotemporal distribution of the solute's concentration in the mobile phase $c_{a,m}$.

III. NONLINEAR SIMULATIONS

Introducing the stream function $\psi(x,y)$, such that $u=\partial\psi/\partial y$ and $v=-\partial\psi/\partial x$, and following Tan and Homsy,[22] the momentum and concentration equations become

$$\nabla^2\psi=-R\left(\frac{\partial\psi}{\partial x}\frac{\partial c}{\partial x}+\frac{\partial\psi}{\partial y}\frac{\partial c}{\partial y}+\frac{\partial c}{\partial y}\right), \tag{14}$$

$$\frac{\partial c}{\partial t}+\frac{\partial\psi}{\partial y}\frac{\partial c}{\partial x}-\frac{\partial\psi}{\partial x}\frac{\partial c}{\partial y}=\frac{\partial^2 c}{\partial x^2}+\epsilon\frac{\partial^2 c}{\partial y^2}, \tag{15}$$

$$(1+k')\frac{\partial c_{a,m}}{\partial t}+\left(\frac{\partial\psi}{\partial y}-k'\right)\frac{\partial c_{a,m}}{\partial x}-\frac{\partial\psi}{\partial x}\frac{\partial c_{a,m}}{\partial y}=\delta\left[\frac{\partial^2 c_{a,m}}{\partial x^2}+\epsilon_a\frac{\partial^2 c_{a,m}}{\partial y^2}\right]. \tag{16}$$

Equation (14) is obtained by eliminating the pressure gradient by taking the curl of Darcy's law. Note that in absence of adsorption ($k'=0$) and for a solute dispersing at the same rate as the sample solvent ($\delta=1$ and $\epsilon_a=\epsilon$), we recover the classical theoretical model of miscible VF studied previously by many authors.[1,12,22,23] The dynamics of the concentration of the sample solvent c and of the solute $c_{a,m}$ then evolve exactly the same way and the dynamics of $c_{a,m}$ is merely that of a passive scalar advected by fingering between the displacing fluid and the sample solvent of the sample. The objective here is to analyze the effect of k', i.e., see how the dynamics of the sample solvent and of the solute can disentangle because of adsorption.

Equations (14)–(16) are numerically solved using the pseudospectral method introduced by Tan and Homsy.[22] The code has been validated here by reproducing the results of Tan and Homsy[22] after reducing the three component system

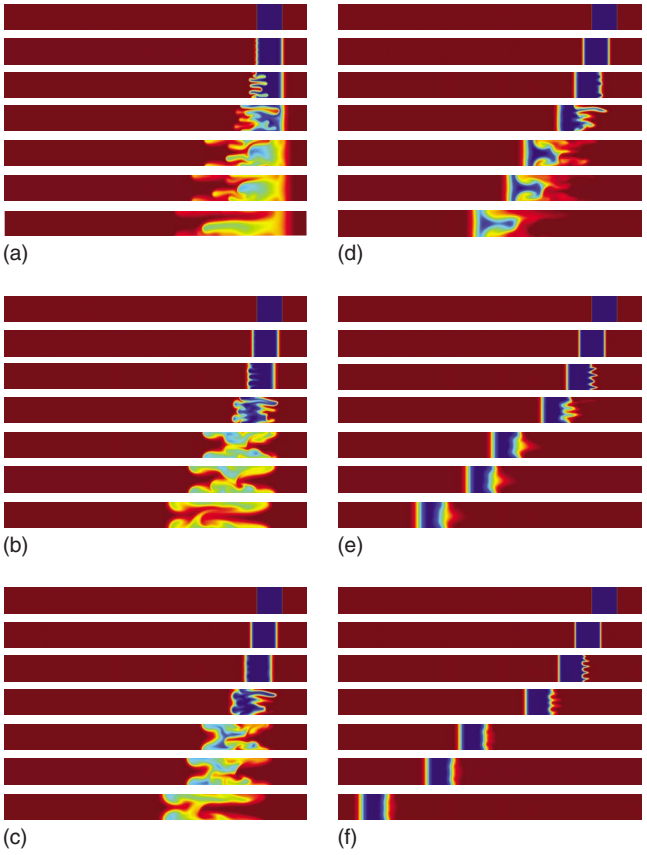

FIG. 2. (Color online) Density plots of the mobile phase concentration of the solute $c_{a,m}$ at successive times in a frame moving at the injection velocity with $L'=512$, $\epsilon=1$, $\delta=1$, $\epsilon_a=1$, $l=512$, and $R=2$; (a) $k'=0$, the dynamics corresponds to the VF dynamics of the sample solvent concentration, (b) $k'=0.2$, (c) $k'=0.3$, (d) $k'=0.5$, (e) $k'=1$, and (f) $k'=2$. From top to bottom: $t=0,500,1000,2000,4000,5000,7000$.

to a two component one by choosing $k'=0$, $\delta=1$, and $\epsilon_a=\epsilon$. Its convergence has also been tested in the case of finite sample fingering.[12]

The boundary conditions are periodic in both x and y directions. Along the axial coordinate x, this is no problem as long as the fingers extending to the left do not interact with the right of the sample by periodicity and vice versa. Periodicity along y is standard for such pattern formation studies.[12,22] In dimensionless units, the length and width are $L=UL_x/D_x$ and $L'=UL_y/D_x$, respectively, while the dimensionless initial length of the sample is $l=UW/D_x$. The initial conditions for both c and $c_{a,m}$ correspond to a convectionless fluid embedding a rectangular sample of concentration $c=1$, $c_{a,m}=1$ and of size $L'\times l$ in a $c=0$, $c_{a,m}=0$ background. The middle of the sample is initially located at $x=4L/5$. The lateral sides of the sample correspond to two back to back step functions between $c=0$ and $c=1$ or between $c_{a,m}=0$ and $c_{a,m}=1$ with an intermediate point where $c=c_{a,m}=1/2+Ar$, where r is a random number between 0 and 1 and A is the amplitude of the noise of the order 10^{-3}. This noise is used to trigger the fingering instability on a pertinent computing time.[12]

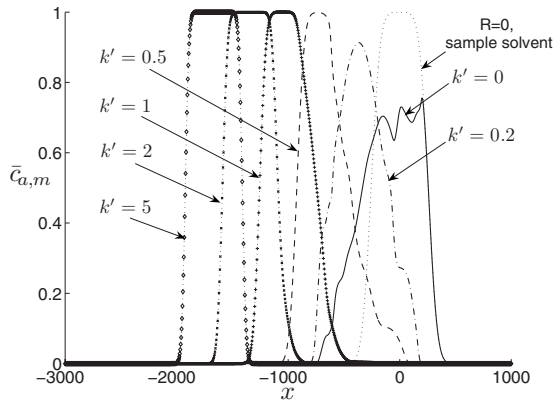

FIG. 3. Transversely averaged concentration profiles of the solute $\bar{c}_{a,m}$ at $t=2000$ for different values of k' and simulations of Fig. 2.

IV. VISCOUS FINGERING IN THE THREE COMPONENT SYSTEM

Density plots of $c_{a,m}$, the concentration of the solute in the mobile phase are plotted at successive times in Fig. 2 for $L'=512$, $l=512$, $\epsilon=1$, $\delta=1$, $\epsilon_a=1$, $R=2$ and different values of the retention parameter k' on a gray scale from black to white corresponding to $c_{a,m}=1$ and $c_{a,m}=0$, respectively (on color, $c_{a,m}=1$ to 0 correspond to blue and red). The system is shown in a frame of reference moving with the injection speed of the eluent. The figures are plotted with a constant aspect ratio. The VF dynamics due to the unfavorable contrast between the viscosity of the displacing fluid and that of the sample solvent is shown in Fig. 2(a). Such a VF of finite slices in two component systems has already been studied quantitatively in detail before.[11,12,14,17,24] In absence of any adsorption, i.e., for $k'=0$ and $c_{a,s}=0$ the solute remains in the mobile phase and follows the dynamics of the flow as a passive scalar. Its fingering is then the same as that of the sample solvent [Fig. 2(a)]. Figures 2(b)–2(f) show the cases when the solute in the injected sample adsorbs onto the porous matrix (i.e., $k'>0$). It is observed that the VF dynamics of the solvent acts upon the evolution of the solute concentration, $c_{a,m}$. In the presence of adsorption the retained solute zone develops fingers when either one interface or both rear and frontal interfaces of it come in contact with the unstable interface of the sample solvent zone [Figs. 2(b)–2(f)]. This is in agreement with experimental observations in chromatography columns.[10] This retained solute zone disengages from the sample solvent zone without any distortion at any of the two interfaces for larger values of k'.

These above results can be quantitatively analyzed using the transversely averaged profiles of the mobile phase concentration of the solute defined as[12]

$$\bar{c}_{a,m}(x,t)=\frac{1}{L'}\int_0^{L'} c_{a,m}(x,y,t)dy. \tag{17}$$

$\bar{c}_{a,m}(x,t)$ is plotted in Fig. 3 for different values of the retention parameter k' at a fixed time $t=2000$ for the nonlinear dynamics of Fig. 2. The reference $x=0$ position along the x-axis is set such that the center of an unretained analyte

zone would occupy at that position in absence of VF. If $R=0$, no fingering occurs and $\bar{c}_{a,m}$ evolves only via dispersion. If $R=2$ but $k'=0$ the curve corresponding to this nonadsorptive case shows the characteristic bumps and the broadening due to the VF dynamics induced by the difference in viscosity of the sample solvent and of the displacing fluid.[12,14,17] When adsorption is occurring ($k' \neq 0$) it is observed that as k' increases, the solute zone is retarded with regard to the sample solvent zone. For some k', both the rear and frontal interfaces get distorted (see the dotted curve for $k'=0.2$) since both rear and frontal interfaces of the solute concentration field are affected by VF of the sample solvent zone given by the curve with $k'=0$. For larger values of k' both rear and frontal interfaces of the solute plug remain nondeformed. This occurs when the solute plug gets disengaged from the solvent plug before VF has had time to disperse the sample solvent. The solute transversely averaged profiles feature then the standard error function characteristic of simple dispersion.

To understand the conditions for a disengagement without distortion of the retained solute zone from the solvent zone, let us discuss in Sec. IV A a simplified model for three component systems.

A. Dispersive model of disengagement of solute zone from sample solvent zone

The three component system is here considered in the case of isoeluotropic sample solvents for which the retention factor k' of the solute is the same in both the sample solvent and the eluent. It is assumed that a rectangular plug of a given sample solvent containing a dissolved solute occupies initially a length L_{inj} of the porous medium. Because the solute is retained on the porous matrix, it moves along the column more slowly than the zone of the unretained sample solvent concentration distribution. From Eqs. (14)–(16), it is clear that, for the case of a stable displacement obtained when $R=0$ and $\psi=0$, the center of mass of the solute plug propagates toward the left of the sample plug with a speed $k'/(1+k')$ in the nondimensional moving frame of reference and with a speed $1/(1+k')$ in the nondimensional steady frame of reference [which corresponds to the dimensional speed $U/(1+k')$]. It is of interest to find the critical time, t_{crit}, at which the solvent zone and the solute zone will cease to overlap. This time can be obtained analytically in the pure dispersive case, in the absence of VF.

In that case indeed, the solute and solvent concentration distributions will cease to overlap when the position of the rear interface of the sample solvent, $x_{s,r}$, will be ahead of the frontal interface of the solute zone, $x_{a,f}$. In a pure dispersive regime, the widths of the solute as well as of the sample solvent zones change in time from their initial dimensional width W to their corresponding dispersive widths. By assuming that all the values of the normal distribution in the pure dispersive displacement lie within two standard deviations (2σ) of the mean, the upstream end of the rear interface of the sample solvent zone is lagging, by a distance $2\sigma_s(t)$, behind the mean position of this rear interface. The downstream end of the frontal interface of the solute zone is ahead, by a distance $2\sigma_a(t)$, of the mean position of the frontal interface. Here $\sigma_s(t)$ and $\sigma_a(t)$ are the spatial standard deviations that the sample solvent zone and the analyte zone, respectively, would have at time t for vanishing W (Dirac injection pulse).

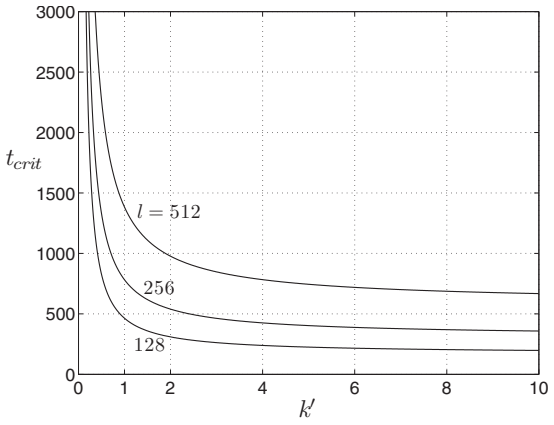

FIG. 4. Dimensionless critical time t_{crit} at which the solute concentration distribution ceases to overlap with the sample solvent one in absence of fingering as a function of k' for different sample lengths l with $\delta=1$.

Assuming that the rear of the sample, at time $t=0$, is at position $x=0$, one has in the steady frame of reference with dimensional quantities,

$$x_{s,r} = Ut - 2\sigma_s(t), \tag{18}$$

$$x_{a,f} = W + \frac{U}{1+k'}t + 2\sigma_a(t), \tag{19}$$

where t is the time elapsed since sample injection and U is the displacing fluid (and sample solvent) velocity. Noting that $\sigma_s(t)=\sqrt{2D_x t}$ and $\sigma_a(t)=\sqrt{2\frac{\delta}{1+k'}D_x t}$, then t_{crit} is the time at which $x_{s,r}=x_{a,f}$, i.e.,

$$Ut_{\text{crit}} - 2\sqrt{2D_x t_{\text{crit}}} = W + \frac{U}{1+k'}t_{\text{crit}} + 2\sqrt{2\frac{\delta}{1+k'}D_x t_{\text{crit}}}. \tag{20}$$

Using $L_c=D_x/U$ and $t_c=D_x/U^2$ as a characteristic length and time as defined before, the dimensionless form of Eq. (20) becomes

$$\frac{k'}{1+k'}t_{\text{crit}} - 2\sqrt{2}\left(1+\sqrt{\frac{\delta}{1+k'}}\right)\sqrt{t_{\text{crit}}} - l = 0, \tag{21}$$

where $l=W/L_c$ as before. Equation (21) gives two roots for $\sqrt{t_{\text{crit}}}$. It can easily be shown that Eq. (21) has a unique solution for all the values of δ only by considering the root with positive sign of square root of discriminant of Eq. (21) and hence the corresponding critical time is

$$t_{\text{crit}} = \left(\frac{1+k'}{k'}\right)^2\left[\sqrt{2}\left(1+\sqrt{\frac{\delta}{1+k'}}\right) + \sqrt{2\left(1+\sqrt{\frac{\delta}{1+k'}}\right)^2 + \frac{k'}{1+k'}l}\right]^2. \tag{22}$$

In Fig. 4 plotting t_{crit} as a function of k' shows that the larger

the retention parameter k', the smaller t_{crit}. Moreover, t_{crit} saturates to an asymptotic value equal to $(\sqrt{2}+\sqrt{2+l})^2$ at larger values of k'. When increasing the initial width of the sample l this asymptotic t_{crit} increases. For $k'=1$, $\delta=1$, and $l=512$ in this pure dispersive case, one can obtain from Eq. (22) that the disengagement of the retained solute and solvent zones occurs at $t=1383$. However, in the presence of VF, this disengagement occurs at a time close to $t=5000$ [see Fig. 2(e)], which is much larger than for the pure dispersive displacement. The presence of VF induces thus a delay in the disengagement of the solute plug from the solvent plug. It means that the unaffected solute zone can be obtained at a later time in the presence of VF than for pure dispersion of sample solvent.

B. Variance of the transverse averaged profile

To quantify the influence of VF on the distortion of the concentration peak of the solute plug, we next compute the variance σ_a^2 of the transversely averaged profiles of concentration $\bar{c}_{a,m}(x,t)$ as[12,14,17]

$$\sigma_a^2(t) = \frac{\int_0^L \bar{c}_{a,m}(x,t)[x-m(t)]^2 dx}{\int_0^L \bar{c}_{a,m}(x,t)dx}, \tag{23}$$

where $m(t)=\int_0^L x f(x,t)dx$ is the first moment of $f(x,t)=\bar{c}_{a,m}(x,t)/\int_0^L \bar{c}_{a,m}(x,t)dx$ which is the probability density function of the continuous distribution $\bar{c}_{a,m}(x,t)$. Similarly a variance σ^2 can be calculated for the solvent plug for transversely averaged profile $\bar{c}(x,t)$ defined along the line above. From Eqs. (15) and (16) the variance σ_o^2 of a stable ($R=0$) solvent peak and the variance $\sigma_{a,o}^2$ of the mobile phase solute peak can be calculated to be $\sigma_o^2=l^2/12+2t$ and $\sigma_{a,o}^2=l^2/12+2[\delta/(1+k')]t$, respectively. The term $l^2/12$ corresponds to the contribution due to the initial width l of the sample, while the term linear in t is due to a dispersive mixing. As done in previous studies of VF of finite slices,[12] when fingering takes place, we can extract the quantity $\sigma_f^2=\sigma^2-\sigma_o^2$ and $\sigma_{a,f}^2=\sigma_a^2-\sigma_{a,o}^2$, which gives the contribution to the total variance σ^2 and σ_a^2 due to VF.

The effects of the adsorption parameter k' on the total variance σ_a^2 are plotted in Fig. 5(a) for the simulations presented in Fig. 2. Similar to the case of VF in two component systems,[12] the variance σ_a^2 increases more in time than $\sigma_{a,o}^2$ because of the widening of the peak due to fingering contributions. However, in the presence of adsorption, the variance reduces as k' increases even if, for small values of $k'<0.3$, the variance does not have a significant different value as the effects of the sample solvent VF are large and the peaks are more distorted. It is clearly observed from Fig. 5(b) that the variance for $k'=1$ or 2 increases only due to dispersion after the time when the solute plug has disengaged from the sample solvent one. Indeed, after a transient increase due to VF the shape of σ_a^2 is again the same as for pure dispersion, i.e., directly proportional to $\sigma_{a,o}^2=l^2/12+2[\delta/(1+k')]t$. The numerical simulation for $R=0$, $k'=1,2$ and the theoretical observation exactly coincide [Fig. 5(b)] which can be considered as a further validation of the present numerical method.

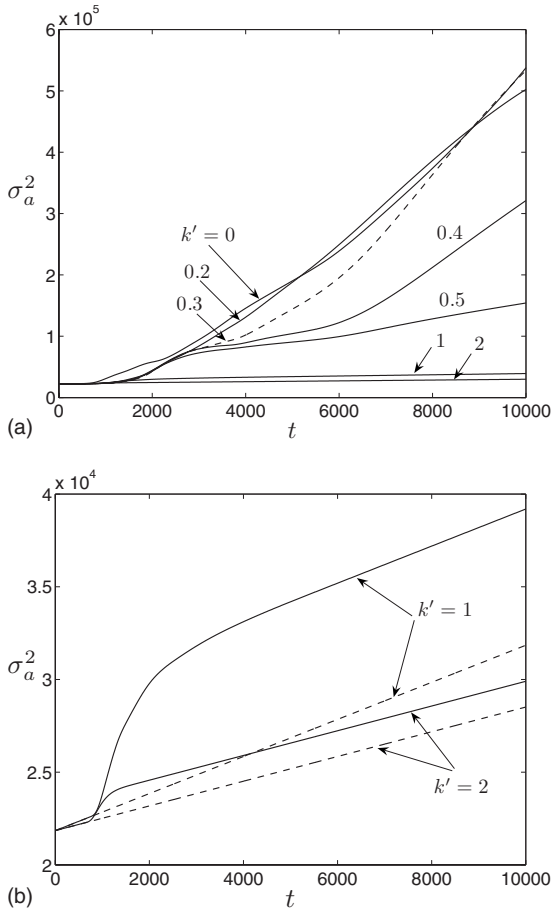

FIG. 5. (a) Variance σ_a^2 of $\bar{c}_{a,m}(x,t)$ as a function of time for different values of k' and simulations of Fig. 2. (b) Enlargement of (a) for $k'=1,2$ and $R=2$ (solid lines) with comparison of the pure dispersion value $\sigma_{a,o}^2=l^2/12+2[\delta/(1+k')]t$ obtained when $R=0$ (dashed lines).

In order to understand the influence of VF of the sample solvent on the broadening of the solute plug, Fig. 6 shows the contribution to the standard deviation due to fingering, $\sigma_{a,f}$, as a function of time for different values of the retention parameter k'. We know from Ref. 12 that for the solvent plug σ_f starts to deviate from zero at the onset time of VF and next increases with time before saturating to an asymptotic value after some time when dispersion takes over again. Similarly the variance of the solute plug deviates from the same initial constant σ_f of the solvent plug when the solute distribution is deformed by fingering. It saturates to an asymptotic value after some time when the effects of the VF are weakening because of the complete disengagement of the solute and solvent plugs. It is seen from Fig. 6(a) that the time interval between the onset time of fingering and the time of saturation is decreasing with increasing k'. For $k'=0,0.2,0.5$ saturation occurs at a time larger than 10 000 whereas for $k'=1,2,3$ saturation occurs at a time close to 3000, 1500, and 1000, respectively. It shows that the larger k', the quicker the disentanglement between solute and solvent plugs. The onset time of the broadening of the solute plug in presence of VF increases and reaches a maximum for a critical value of k' [here close to $k'=0.5$, see Fig. 6(b)] then starts decreasing for further increasing of k'. It can how-

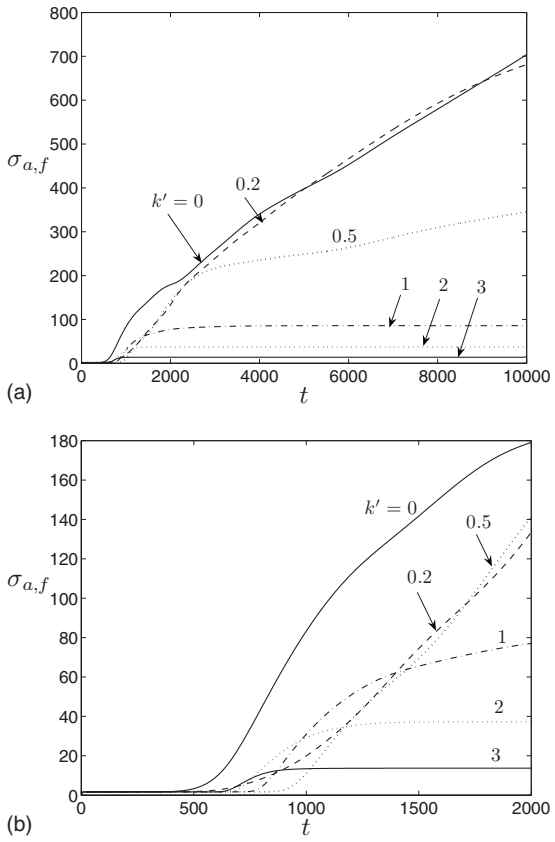

FIG. 6. (a) Contribution of fingering to the standard deviation $\sigma_{a,f}$ as a function of time for different values of k' with $L'=512$, $\epsilon=1$, $\delta=1$, $\epsilon_a=1$, $l=512$, and $R=2$; (b) zoom at early times.

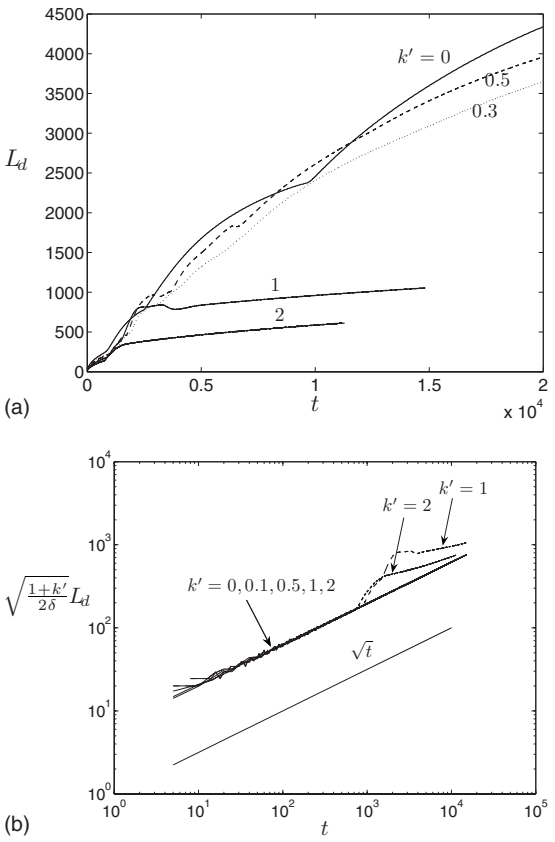

FIG. 7. (a) Spreading length L_d of the solute as a function of time for the simulations of Fig. 2 and different values of k'. (b) Corresponding log-log plots for the pure dispersive case ($R=0$; solid lines) and comparison with the $R=2$ (dashed lines) cases with retention. The curve with label $\sqrt{t}$ is to show the characteristic slope corresponding to the pure diffusion.

ever not be smaller than the onset time of the solvent VF or, in other words, than the onset time for the non adsorptive solute displacement.

It is observed that for some cases, for example, Fig. 2(e) at $t>4000$, a distortion at the frontal interface, which can be due to the interaction of that interface with VF at an earlier time, can remain for quite a long time before being smoothed out by dispersion. This phenomenon can also be seen in Fig. 6(a) for $k'=1$ where the saturation of the variance to an asymptotic value is already achieved at $t=4000$, i.e., the broadening is only due to the dispersion.

C. Spreading length of solute zone

The mixing length which is nothing else but the length of the fingering zone is an important measure in the study of VF as it gives information on the length of the zone where the two miscible fluids mix with each other.[12,17] Similarly, in order to understand the length of the displacement of the solute zone due to VF, we quantify the spreading of solute fingers by the length l_d of the interval in which $\bar{c}_{a,m}(x,t)>10^{-3}$. The evolution of the spreading length of the solute defined as $L_d=l_d-l$ is plotted for different retention parameters k' in Fig. 7(a). It shows that at lower k', the length of the solute displacement zone have similar trends whereas at large k', the length L_d decreases for increasing k'. Figure 7(b) depicts the evolution of L_d normalized by $\sqrt{2\delta/(1+k')}$ for different k' without the effects of VF (i.e., for pure dispersion when $R=0$) through a log-log plot. It shows that in a pure dispersion regime, the displacement length is the same for all k'. The normalized length $\sqrt{2\delta t/(1+k')}$ is the standard deviation of the solute concentration profile which can be found by solving the linear part of Eq. (12). It is seen that the displacement length evolves then proportionally to $\sqrt{t}$. Figure 7(b) shows that for $R=2$, $k'=1$ and 2, after the solute band interacted with VF and completely disentangled from the VF zone the displacement of the solute is dominated again by dispersion. However this dispersion of the solute band is not directly proportional to $\sqrt{t}$ like in a pure dispersive case, rather it moves with a power of t which is less than 0.5. It is interesting to note that the effects of VF reduce the power-law relationship of the dispersion length of the solute with time.

D. Parametric study

It is well known that the larger the value of the log-mobility R, the more intense VF and the faster the fingers travel.[12,14,22] From Fig. 8(a) we find that VF with $R=3$ affects the broadening of solute plug for larger values of the retention parameter k' than for $R=2$ (shown in Fig. 6), i.e., the time needed for a disengagement process reduces for larger values of k'. So, at fixed R, there is a critical k' above which the broadening of the solute plug is not affected by

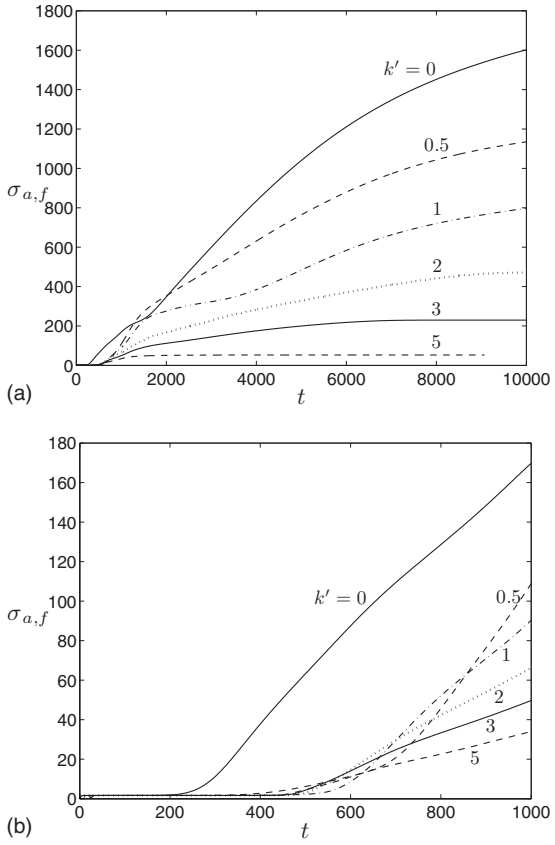

FIG. 8. (a) Same as Fig. 6 except for $R=3$; (b) zoom at early times.

VF. This critical k' increases with increasing R. As a corollar, the time during which the solvent and solute plugs interact increases for a fixed k' as R increases. The onset of fingering on the solute plug occurs early for large R, which is seen from Fig. 8(b), as for $k'=0.5$ the onset time of solute fingers for $R=2$ is close to $t=900$ [see Fig. 6(b)] and for $R=3$ it is nearer to $t=400$. For $R=3$, the onset time of fingering of the solute plug first increases with increasing k', then reaches a maximum for a critical k' close to 1. This critical k' is larger than in the $R=2$ case [see Fig. 6(b)] where it was found to be close to 0.5. Furthermore, it is observed that for larger R, the fingering variance takes a longer time to reach an asymptotic value for a fixed k', which reveals that fingers travel faster for large R.

On the other hand, decreasing the ratio of dispersion coefficients $\epsilon=D_y/D_x$ for a fixed value of R has a destabilizing effect and the sample solvent VF is more intense.[12] As a consequence decreasing ϵ leads to a stronger influence of VF on the displacement of the solute zone. Since small transverse dispersion D_y favors longitudinal growth of VF by allowing the fingers to survive for a longer time, the solute zone needs a longer time to disentangle from the solvent plug and be unaffected by VF. This can be seen from a comparison of Figs. 6 and 9 for different values of k'. For $k'=2$ the critical time $t_{\text{crit}}\sim 3000$ when $\epsilon=0.2$ as compared to $t_{\text{crit}}=1500$ for $\epsilon=1$ in Fig. 6. So, for small dispersion ratio ϵ, the critical k' above which the solute plug is unaffected by VF at anytime increases. Similarly this critical k' will increase for larger L' as the VF is then more intense too.

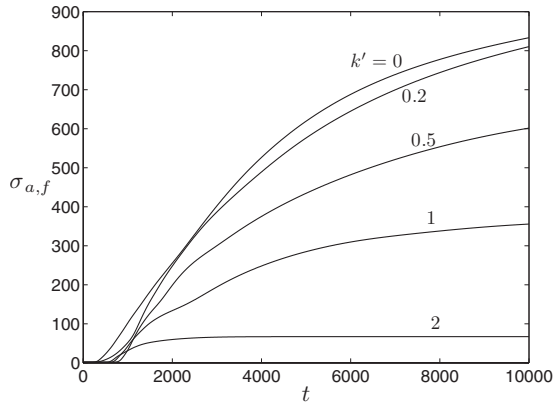

FIG. 9. Same as Fig. 6 except for $\epsilon=0.2$.

Figure 10 shows the influence of the initial sample length l on the broadening of the solute zone in presence of sample solvent VF. The larger the initial extent of the sample, the larger the mixing zone between the sample solvent and the displacing fluid. Hence the VF zone interacts longer with the solute zone thereby increasing the broadening of $\sigma_{a,f}$. The smaller l for a fixed k', the faster the solute zone disentangles from the sample solvent zone, hence the faster the temporal dependence of $\sigma_{a,f}$ reaches a plateau, as seen in Fig. 10. The critical k' for the disengagement of both zones increases with increasing sample length l.

Eventually, Fig. 11 shows the influence on $\sigma_{a,f}$ of the ratio of the longitudinal dispersion coefficients $\delta=D_{a_x}/D_x$ of the solute in the mobile phase and of the sample solvent. For larger values of δ, VF of the solvent affects $\sigma_{a,f}$ during a longer time. Saturation of $\sigma_{a,f}$ occurs therefore at a later time for increasing δ. The onset of the broadening of the solute zone due to VF occurs quicker for increasing δ as seen in Fig. 11(b). This is due to the fact that a larger value of δ implies larger axial dispersion of the solute zone favoring the longitudinal growth of the solute concentration distribution. This allows the solute to interact on longer distances and for a longer time with the VF of the sample solvent.

In spite of this augmented duration of the interaction between the analyte and sample zones, which allows more time for the analyte zone to be affected by the VF process on

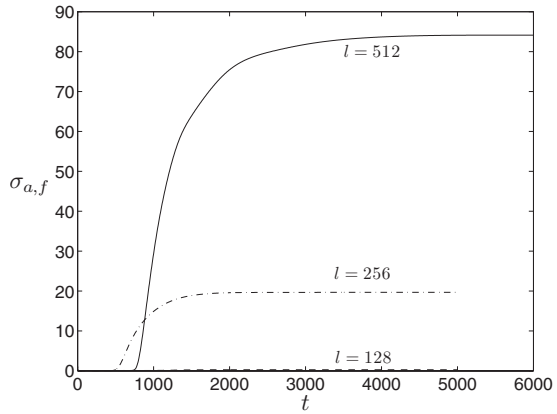

FIG. 10. $\sigma_{a,f}$ as a function of time for different values of the initial sample length l for $L'=512$, $\epsilon=1$, $\delta=1$, $\epsilon_a=1$, $R=2$, and $k'=1$.

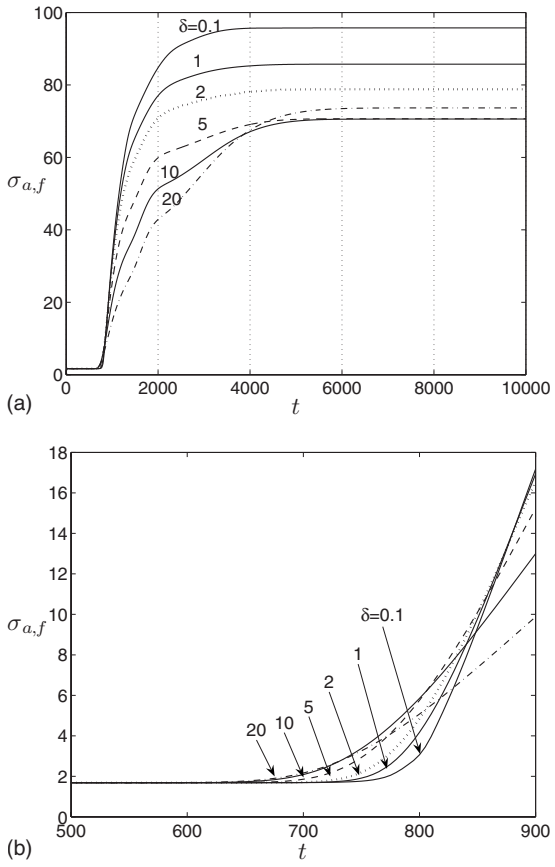

FIG. 11. (a) Effects of fingering on $\sigma_{a,f}$ as a function of time for different values of δ with $L'=512$, $\epsilon=1$, $k=1$, $\epsilon_a=1$, $l=512$, and $R=2$; (b) zoom at early times.

the upstream side of the sample solvent zone, the saturation value of $\sigma_{a,f}$ is observed to decrease on increasing delta in Fig. 11(a). In fact, as the axial dispersion of the analyte increases, its transverse dispersion also increases since ϵ_a is here kept equal to 1. This promotes a faster merging of the fingers of the analyte zone and a resulting lower VF contribution to the standard deviation of this zone. This finding illustrates the significant role played by transverse dispersion for limiting the VF effect.

V. CONCLUSION

When a passive solute undergoing adsorption on the porous matrix is initially dissolved in a solvent which is more viscous than the displacing fluid, its transport properties can be affected by VF phenomena taking place at the interface where the carrier fluid displaces the sample solvent. The dynamics of the solute concentration has been characterized here in such conditions on the basis on numerical simulations of a three component model consisting in Darcy's law coupled to the evolution equation for the solute and solvent concentrations, this latter one controlling the viscosity of the solution. If the solute is unretained and diffuses at the same rate as the solvent, the solute is merely a passive scalar following the fingering taking place between the displacing fluid and the solvent. If the solute is, on the contrary, retained on the porous matrix, its dynamics can more or less disentangle from the fingering area depending on the strength of the retention factor k'. The concentration peak of the solute can, in that case, feature deformations due to the fingering processes either on its back, on both frontal and rear interfaces, or only on the frontal part depending whether k' is small, of intermediate value or large. Nondeformed peaks of solute distribution are obtained above a critical value of k' when the solute plug rapidly disentangles from the solvent one before fingering has had time to act. The critical time at which this disentanglement takes place has been calculated analytically in the pure dispersion case and has been shown to be smaller than the disentanglement time when fingering takes place. A parametric study furthermore shows that this critical time is an increasing function of the log-mobility ratio R and of the initial length l of the sample but a decreasing function of the ratio of dispersion coefficients ϵ of the solvent. Moreover if the ratio δ between the axial dispersion coefficient of the solute and that of the solvent is increased, the solute interacts on longer distances with the fingering which increases therefore the broadening of the solute peak. These results are in agreement with recent experimental findings in chromatography columns.[10]

ACKNOWLEDGMENTS

M.M. from ULB gratefully acknowledges a postdoctoral fellowship of the FRS-FNRS (Fonds de la Recherche Scientifique), Belgium. A.D. acknowledges financial support from the Communauté Française de Belgique (Actions de Recherches Concertées Programme), Prodex and FNRS. The collaboration between our ULB and ESPCI teams is financially supported by a French (Programme d'Actions Intégrées under Contract No. 08948YD) and Belgian (CGRI) Tournesol grant.

[1] G. M. Homsy, "Viscous fingering in porous media," Annu. Rev. Fluid Mech. **19**, 271 (1987).
[2] S. Hill, "Channeling in packed columns," Chem. Eng. Sci. **1**, 247 (1952).
[3] P. G. Saffman and G. I. Taylor, "The penetration of a fluid into a porous medium or Hele-Shaw cell containing a more viscous liquid," Proc. R. Soc. London, Ser. A **245**, 312 (1958).
[4] M. Czok, A. Katti, and G. Guiochon, "Effect of sample viscosity in high-performance size-exclusion chromatography and its control," J. Chromatogr. A **550**, 705 (1991).
[5] E. J. Fernandez, T. Tucker Norton, W. C. Jung, and J. G. Tsavalas, "A column design for reducing viscous fingering in size exclusion chromatography," Biotechnol. Prog. **12**, 480 (1996).
[6] D. Cherrak, E. Guernet, P. Cardot, C. Herrenknecht, and M. Czok, "Viscous fingering: A systematic study of viscosity effects in methanol-isopropanol systems," Chromatographia **46**, 647 (1997).
[7] M. L. Dickson, T. T. Norton, and E. J. Fernandez, "Chemical imaging of multicomponent viscous fingering in chromatography," AIChE J. **43**, 409 (1997).
[8] B. S. Broyles, R. A. Shalliker, D. E. Cherrak, and G. Guiochon, "Visualization of viscous fingering in chromatographic columns," J. Chromatogr. A **822**, 173 (1998).
[9] H. J. Catchpoole, R. A. Shalliker, G. R. Dennis, and G. Guiochon, "Visualising the onset of viscous fingering in chromatography columns," J. Chromatogr. A **1117**, 137 (2006).
[10] S. Keunchkarian, M. Reta, L. Romero, and C. Castells, "Effect of sample solvent on the chromatographic peak shape of solutes eluted under reversed-phase liquid chromatographic conditions," J. Chromatogr. A **1119**, 20 (2006).
[11] G. Rousseaux, A. De Wit, and M. Martin, "Viscous fingering in packed chromatographic columns: Linear stability analysis," J. Chromatogr. A **1149**, 254 (2007).

[12]A. De Wit, Y. Bertho, and M. Martin, "Viscous fingering of miscible slices," Phys. Fluids **17**, 054114 (2005).
[13]V. Kretz, P. Berest, J.-P. Hulin, and D. Salin, "An experimental study of the effects of density and viscosity contrasts on macrodispersion n porous media," Water Resour. Res. **39**, 1032, DOI: 10.1029/2001WR001244 (2003).
[14]M. Mishra, M. Martin, and A. De Wit, "Differences in miscible viscous fingering of finite width slices with positive and negative log-mobility ratio," Phys. Rev. E **78**, 066306 (2008).
[15]G. R. Johnson, Z. Zhang, and M. L. Brusseau, "Characterizing and quantifying the impact of immiscible-liquid dissolution and nonlinear, rate-limited sorption/desorption on low-concentration elution tailing," Water Resour. Res. **39**, 1120, DOI: 10.1029/2002WR001435 (2003).
[16]S. E. Serrano, "Propagation of nonlinear reactive contaminants in porous media," Water Resour. Res. **39**, 1228, DOI: 10.1029/2002WR001922 (2003).
[17]M. Mishra, M. Martin, and A. De Wit, "Miscible viscous fingering with linear adsorption on the porous matrix," Phys. Fluids **19**, 073101 (2007).
[18]G. Guiochon, A. Felinger, D. G. Shirazi, and A. M. Katti, *Fundamentals of Preparative and Nonlinear Chromatography* (Elsevier, San Diego, 2006).
[19]C.-Y. Chen and E. Meiburg, "Miscible displacement in capillary tubes: Influence of Korteweg stresses and divergence effects," Phys. Fluids **14**, 2052 (2002).
[20]H. H. Hu and D. D. Joseph, "Miscible displacement in a Hele-Shaw cell," Z. Angew. Math. Phys. **43**, 626 (1992).
[21]P. Petitjeans and T. Maxworthy, "Miscible displacement in capillary tubes. Part 1. Experiments," J. Fluid Mech. **326**, 37 (1996).
[22]C. T. Tan and G. M. Homsy, "Simulation of nonlinear viscous fingering in miscible displacement," Phys. Fluids **31**, 1330 (1988).
[23]C. T. Tan and G. M. Homsy, "Stability of miscible displacements in porous media: Rectilinear flow," Phys. Fluids **29**, 3549 (1986).
[24]C.-Y. Chen and S.-W. Wang, "Miscible displacement of a layer with finite width in porous media," Int. J. Numer. Methods Heat Fluid Flow **11**, 761 (2001).